Journal of Applied Fluid Mechanics, Vol. 18, No. 9, pp. 2226-2238, 2025.
Available online at www.jafmonline.net, ISSN 1735-3572, EISSN 1735-3645.
https://doi.org/10.47176/jafm.18.9.3209

Computational Fluid Dynamics Studies on a Centrifugal Compressor Stage with Twisted Vanes of a Low Solidity Diffuser

P. Venkateswara Rao [1†], V. R. Govindaraju[2], K. Venkateswarlu[3], and M. Bhanu Kumari [4]

[1] *Department of Mechanical Engineering, Vasavi College of Engineering, Hyderabad, Telangana, India*
[2] *Turbomachinary, BHEL, Vikasnagar, Hyderabad 500093, India*
[3] *Mechanical and Metallurgical Engineering, School of Engineering and the Built Environment, JEDS Campus, University of Namibia, Private Bag 3624, Ongwediva, Namibia*
[4] *Department of Mathematics, Lords College of Engineering and Technology, Hyderabad, India*

†Corresponding Author Email: p.v.rao@staff.vce.ac.in

ABSTRACT

This study examines the effect of a twisted diffuser vane on the performance of a centrifugal compressor stage. A computational analysis was conducted to assess how the setting and twist angles influence the compressor's performance and diffuser static pressure recovery (SPR). The diffuser vane was modeled using a standard aerofoil design with minor adjustments to the trailing edge. A twisted diffuser blade was created by varying the twist angle from hub to shroud, which results in different stagger angles. Three types of diffusers—vaneless, low solidity vaned, and twisted vaned—were analyzed across five flow coefficients. The results show that adding twist to the diffuser vane improves both the compressor stage efficiency and its operating range at a 24° setting angle, regardless of the twist angle. The highest efficiency occurs at the design flow coefficient for all twist angles considered. However, the SPR coefficient increased for twist angles of 9° and 11° up to the 24° setting angle, and decreased at setting angles of 28° and 32°. Based on the selected impeller-diffuser configuration, the optimal twist angle for maximum performance was found to be 9° at a 24° setting angle.

Article History

Received November 27, 2024
Revised March 31, 2025
Accepted April 11, 2025
Available online July 5, 2025

Keywords:

Centrifugal compressor
Mach number
Stagger angle
Twist
Diffuser

1. INTRODUCTION

A compressor is a type of turbomachine that applies pressure to a fluid by using power. Continuous-flow, rotating devices known as dynamic compressors use a fast-spinning element to accelerate air and transform its velocity head into pressure in the revolving element as well as in stationary diffusers or blades (Engeda, 2001). The diffuser slows down the fluid, converting kinetic energy into static pressure. Centrifugal compressors are widely used in industries such as fertilizers, petrochemicals, refrigeration, air conditioning, aerospace, automotive, and various process industries. The type of diffuser used determines the compressor's stable operating range and pressure rise.

At the impeller outlet, non-uniform flow conditions can arise, where the centrifugal impeller's output flow interacts with the diffuser's vaneless area. This interaction increases static pressure but significantly reduces total pressure, contributing to inefficiency. Understanding the relationship between the stationary diffuser and the rotating impeller is crucial for improving centrifugal compressor performance. Efforts to enhance compressor efficiency have focused on modifying the geometry of the diffuser, return channel, and impeller.

The impeller's shape, a key active component that imparts energy to the fluid, greatly affects compressor performance. Advances such as the use of splitter blades (Higashimori et al., 2004), tandem blades (Larosiliere et al., 1997 and Roberts & Kacker, 2002), and three-dimensional impeller designs (Zangeneh, 1991, 1998) have led to significant improvements. Altering impeller geometry impacts the intake and exit velocity triangles, potentially leading to substantial changes in performance. Research has shown that adding skew (lean) to the impeller blades can enhance performance (Moore & Moore, 1994).

The diffuser plays a critical role in transforming kinetic energy into static pressure in centrifugal compressors. The demand for improved efficiency, a stable operating range, and higher pressure ratios in centrifugal compressors has increased. The choice of diffuser

Nomenclature

C_p	static pressure recovery coefficient	α	flow angle
D	diameter	β	blade angle
g	acceleration due to gravity	η	total-to-static stage efficiency
H	total head	λ	power coefficient
l	vane chord length	ω	angular velocity
LE	leading Edge	ϕ	flow coefficient
LSVD	Low Solidity Vaned Diffuser	γ	ratio of specific heats
M	mass flow rate	ρ	inlet density
N	speed	σ	solidity
p	pressure	ψ	head coefficient
r	radius	**SUBSCRIPTS**	
R	gas constant	0	total quantities
S	pitch	1	impeller inlet
TVD	Twisted Vaned Diffuser	2	impeller exit
u	peripheral velocity	3	diffuser inlet
VLD	Vaneless diffuser	4	diffuser exit
Z	number of diffuser vanes		

type influences these aspects. A vaneless diffuser is typically used when low cost and a wide operating range are priorities, while a vaned diffuser is used to achieve higher efficiency and pressure rise, often at the cost of operating range.

Recent research by Wu et al. (2024) optimized the diffuser design using NURBS curves and axisymmetric hub shapes. This optimization increased the stall margin from 12.8% to 20.4% and boosted peak efficiency by 0.78%. Analysis showed that the vaneless and semi-vaneless areas of the diffuser reduced recirculation and mixing losses, improving performance at the highest efficiency point.

In addition to traditional diffusers, two other types have gained popularity: partial vaned diffusers (PVD) and low solidity vaned diffusers (LSVD). These diffusers offer a balance between conventional vaned diffusers (CVND) and vaneless diffusers (VLD) in terms of performance. In a centrifugal compressor, the diffuser contributes to about two-thirds of the total losses.

As the demand for high-efficiency machinery increases, the CVND has become essential in centrifugal compressor stage design. However, designers often face challenges with a limited stable operating range when using CVND due to issues like vane throat choke at high mass flows and vane stall at low mass flow rates (MFRs). This has led to the development of new vaned diffuser designs or alternative matches to meet customer requirements (Senoo et al., 1983). In response, several researchers have explored the use of LSVDs in various centrifugal compressors, aiming to understand the influence of incidence angle, vane number, and leading-edge radius ratio on stage performance. Osborne and Sorokes (1988) showed that LSVDs could be applied to centrifugal compressors operating at different speeds, using the Senoo model for their design, although their diffuser blades were simple flat-plate vanes.

Eynon and Whitfield (1997) studied the effects of turning angle and diffuser vane number on system performance and found that varying the number of diffuser vanes had no impact on performance. However, they observed that increasing the vane turning angle resulted in a higher peak pressure ratio and a higher maximum MFR, indicating that the turning angle significantly influenced performance. Senoo (1984) outlined the ways in which solidity, stagger angle, and vane number affect LSVD performance, emphasizing the contribution of secondary flow to increased diffuser efficiency. In order to examine how solidity and vane number affect stage performance, Amineni and Engeda (1997) investigated four LSVDs downstream of the same impeller. Their tests, which also compared a vaneless and a standard vaned diffuser, showed that the pressure recovery in LSVDs was comparable to that of traditional vaned diffusers. Amineni et al., (1996) used three-dimensional viscous simulations to explore flow dynamics in low solidity vaned diffusers. They found that when end-wall separation coincided with vane suction-side separation, poor solidity vaned diffusers experienced stalls. Their study concluded that design factors such as solidity, incidence angle, and blade turning angle significantly affect diffuser performance.

In the diffuser system of a transonic centrifugal compressor, Hayami et al. (1990) transformed high-stagger linear cascades of double-circular-arc vanes into low-solidity circular cascades with a solidity of 0.69. Even at Mach numbers exceeding unity, these circular cascade diffusers showed excellent pressure recovery over a wide range of flow angles.

Liu et al. (2023) developed a multi-objective optimization design platform to assess the effects of solidity and blade aspect ratio on heavy-duty gas turbine transonic compressor performance. By applying a blade parameterization approach, Kriging surrogate model, and NSGA-II optimization method, they demonstrated that the total pressure ratio, isentropic efficiency, and stall margin could be improved by 0.96% and 18.7%, respectively, under design conditions with a constant MFR.

The study of Yang and Liu (2023) presents a novel vane diffuser that is intended to work with an impeller that has a high pressure ratio. The diffuser achieves a twisted shape for the vane and hub by employing a special design

technique that produces transitions from a two-dimensional meridian to a three-dimensional configuration. The axial, bend, and radial sections eventually combine to produce an integrated vane arrangement. When compared to a traditional vaned diffuser, the new diffuser drastically lowers the compressor's overall radial dimension.

Engeda (2001) made significant contributions to the development of new diffuser systems, notably the creation of low solidity vaned diffusers (LSVDs). These diffusers represent a compromise between efficiency and operating range. Issac et al. (2004) investigated the performance of a centrifugal compressor with a PVD. After comparing the performance of PVDs, flat plate diffusers, and VLDs, they resolved that VLDs outperformed the others. Reddy et al. (2004, 2007) explored the influence of vane breadth and vane setting angle on the performance of LSVDs. Their studies demonstrated that these factors significantly affect the stage performance of these devices. LSVDs with an aerofoil vane profile were found to operate effectively across a wide range of flow incidences.

Abdelwahab (2005a,b; 2007) and Abdelwahab & Gerber (2008) explored the use of cambered NACA 65 airfoil profiles that provide a twist in the impeller's rotational direction. Their research demonstrated that using different chord lengths for the hub and shroud and incorporating a three-dimensional airfoil diffuser helped create more consistent blade loading by reducing secondary flows near the diffuser's suction surface. Beach et al. (2024) conducted experimental research on the effects of inlet guide vane re-staggering on stall behavior in high-pressure axial compressors. Their findings revealed that while re-staggering altered the stage matching, it did not change the stall inception process.

Further studies by Venkateswara Rao et al. (2013b, 2014a,b) and Venkateswara Rao and Ramana Murty (2013) demonstrated that twisted vanes in diffusers enhance centrifugal compressor performance.

Although impeller efficiencies in modern compressors are typically around 90%, further improvements are limited by mechanical constraints in blade design. To improve overall performance, attention has shifted toward diffuser design, which faces fewer constraints. While impeller efficiency remains high, diffuser efficiency typically ranges between 65-75%, limiting the overall compressor efficiency to around 80%. Increasing diffuser efficiency by 4-5% could significantly boost compressor performance.

This study compares the performance of a particular impeller using three types of diffusers: vaneless diffuser (VLD), twisted vane diffuser (TVD), and low solidity vane diffuser (LSVD). A standard uncambered aerofoil profile (NACA0010) is used to create the diffuser vane, with minor adjustments made to the trailing edge. A twisted diffuser blade and staggered angles are produced by varying the twist angle from hub to shroud. From hub to shroud, the chord length stays constant, and a number of setting angles between 16° and 32° (in 4° increments)

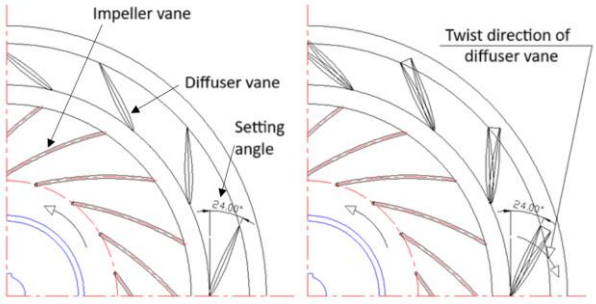

(a) LSVD (b) TVD

Fig. 1 Schematic arrangement of diffusers LSVD & TVD

are quantitatively examined. The twist angle of the diffuser vane is varied from 5° to 11°, with 2° steps, at each setting angle. The schematic arrangement of impeller and diffuser vane at 24° (LSVD) and twisting of diffuser vane at 24° is shown in Fig. 1.

The computational models for VLD, LSVD, and TVD setups include diffuser vane and impeller blade passages. CFD simulations were performed at 4500 rpm with twist applied both in the direction of the impeller's rotation and in the opposite direction. The results showed that performance was enhanced when the twist was applied opposite to the impeller's rotation. Applying twist in the same direction as the impeller's rotation causes significant negative incidence on the blades, leading to reduced diffuser performance. Therefore, in the twisted vaned diffuser configurations, the twist is oriented opposite to the impeller's rotational direction.

2. NUMERICAL INVESTIGATIONS

A typical industrial compressor stage is selected for the present study. Table 1 provides the compressor parameters. Five distinct flow coefficients are used in the study for the diffusers VLD, LSVD, and TVD. These include the design MFR, two flow coefficients below the design MFR (80% and 90%), and two above the design MFR (110% and 120%).

2.1 Details of the CFD Model

Since both the diffuser and impeller have a cyclically symmetric shape, numerical simulations were conducted on a single stage passage at a time using periodic boundary conditions. This approach minimized computational time and reduced the model size. The diffuser serves as a stationary domain, while the impeller operates as a rotating domain. Numerical simulations are performed using a 3-D model to capture the complex behavior of the fluid flow. This approach allows for a more accurate representation of the flow patterns within the system. AutoCAD is used for the geometric modeling of impeller and vaned diffusers. GAMBIT software is used to discretize and simulate the vaneless diffuser. The analysis grid geometries are displayed in Figes 2(a) through (c).

Table 1 Design details of compressor stage

Parameter	Value
Speed, n	4500 rpm
Impeller vane radius at inlet	150 mm
Impeller vane outlet at radius	250 mm
Diffuser vane radius at inlet	275 mm
Diffuser vane radius at outlet	322-344 mm
Impeller width	24.5 mm
Blade angle at impeller inlet, β_1 w.r.t. tangential direction	27°
Blade angle at impeller exit, β_2 w.r.t. tangential direction	45°
Width of the diffuser passage, b	24.5 mm
Mass flow rate, $\dot{m}$	1.3 kg/s
Diffuser blade chord length at hub, l	100 mm
Number of impeller blades	17
Number of diffuser blades, Z	14
Diffuser solidity	0.81

Structured hexahedral grids are created using Turbogrid, guaranteeing high-quality mesh refinement at the leading and trailing edges of the blade. Studies on grid independence are carried out under design flow conditions for the selected configurations. The ideal grid size is determined using the static pressure recovery coefficient (Cp). When comparing the outcomes of the other three grids, the results of grid 4 are used as the benchmark. Table 2 displays the percentage variations in Cp. For every diffuser form under study, grid 3 has the lowest percentage difference in Cp when compared to grids 1 and 2. Grid 3 is therefore employed for additional analysis. The simulation employs a grid with a minimum value of y+ as 2 and a maximum value of y+ as 6, which falls within the acceptable limits (Venkateswara Rao et al., 2014b), as shown in Fig. 3. For the current investigation of the compressor stage, a mixing plane interface is chosen between the impeller exit and the diffuser inlet. This approach enables the generation of steady-state predictions for multi-stage machines.

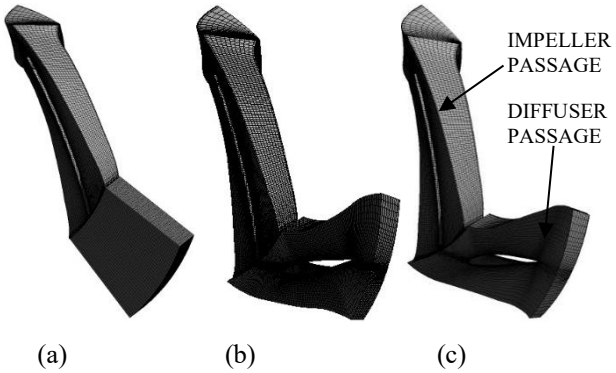

Fig. 2 Compressor stage mesh details, impeller with a) VLD b) LSVD NACA 0010 and c) TVD NACA 2410

2.2 Boundary Conditions

To maintain the inlet boundary condition unaffected by the impeller blade back pressure, the computational domain inlet is positioned ahead of the impeller eye. A uniform total pressure boundary condition is applied at the inlet in the stationary frame, with air entering axially. The simulation uses an absolute pressure of 95,000 Pa, and air is modeled as an ideal gas with an inlet temperature of 310 K.

Table 2 Grid independence study of the compressor stage

Diffuser vane setting angle at hub 24°	Grid	Number of Stage Elements	c_p	% difference
LSVD NACA 0010	Grid1	36856	0.54598	1.882
	Grid2	43240	0.55103	0.974
	Grid3	53682	0.55635	0.018
	Grid4	68258	0.55643	--
TVD NACA 0010 Twist angle 5°	Grid1	37024	0.55982	2.372
	Grid2	43408	0.56676	1.163
	Grid3	54089	0.56982	0.628
	Grid4	69110	0.57343	-
TVD NACA 0010 Twist angle 7°	Grid1	35720	0.56753	1.406
	Grid2	43340	0.57017	0.948
	Grid3	53580	0.57247	0.549
	Grid4	69412	0.57563	-
TVD NACA 0010 Twist angle 9°	Grid1	37680	0.56627	1.439
	Grid2	44300	0.57196	0.449
	Grid3	54920	0.57431	0.041
	Grid4	68540	0.57454	--
TVD NACA 0010 Twist angle 11°	Grid1	35720	0.55209	1.920
	Grid2	44340	0.55852	0.778
	Grid3	53580	0.56090	0.354
	Grid4	69412	0.56290	-

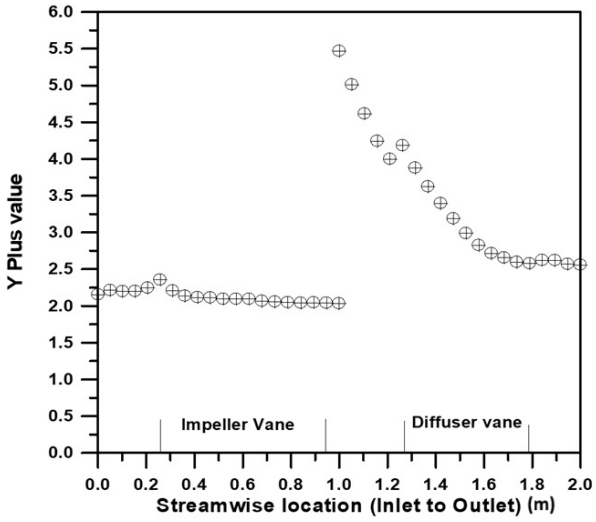

Fig. 3 Variation of y+ value along the stream wise direction in the stage-TVD configuration

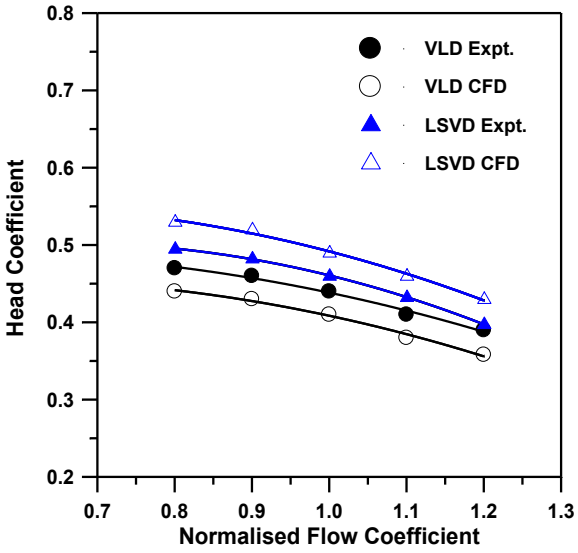

Fig. 4 Variation of head coefficient

The k-ε turbulence model is used for the computations due to its simplicity, lower computational cost, and broad applicability. A rotational periodic boundary condition is implemented to the sidewalls of the impeller and diffuser domains. The specified outlet boundary condition is MFR, and the fluid time step is given by 0.1/ω. The residual error for each governing equation is maintained below 1×10^{-5}.

2.3 Governing Equations

The governing equation in RANS form are

Continuity equation, $\frac{\partial \rho}{\partial t} + \nabla.\left(\rho\overline{C}\right) = 0$ (1)

Momentum equation, $\frac{\partial(\rho\overline{C})}{\partial t} + \nabla.\left(\rho\overline{C}\times\overline{C}\right) =$

$\nabla.\left\{\tau - \overline{\rho C\times C}\right\} + S_M$ (2)

$-\overline{\rho C\times C}$ is the Reynolds stress tensor.

Energy equation,

$\frac{\partial \rho h_{tot}}{\partial t} - \frac{\partial \rho}{\partial t} + \nabla.\left(\rho\overline{C}h_{tot}\right) = \nabla.\left(\lambda\nabla\tau - \overline{\rho Ch}\right) +$
$\nabla.\left(\overline{C}\times\tau\right) + S_E$ (3)

where, the stress tensor (τ) is given by,

$\tau = \mu\left(\nabla\overline{C} + \left(\nabla\overline{C}\right)^T\right) - \frac{2}{3}\delta\nabla.\overline{C}$ (4)

$h_{tot} = h + k$ (5)

k is the turbulent kinetic energy, $k = \frac{1}{2}\overline{C^2}$ (6)

S_M is momentum source and S_E is energy source.

2.4 Formulae Used

Flow coefficient $\emptyset = \frac{Q}{\frac{\pi}{4}D_2^2\times U_2}$ (7)

Total head coefficient, $\psi = \frac{gH}{U_2^2}$ (8)

Total Head $H = \frac{\gamma}{\gamma-1}RT_{01}\left[\left(\frac{p_{04}}{p_{01}}\right)^{\frac{\gamma-1}{\gamma}} - 1\right]\times\frac{1}{g}$ (9)

Total-to-static stage efficiency (%)

$$\eta_{ts} = \left[\left(\frac{p_4}{p_1}\right)^{\gamma/\gamma-1} - 1 \Big/ \left(\frac{T_{04}}{T_{01}} - 1\right)\right]\times 100 \quad (10)$$

Total-to-total efficiency (%) $\eta_{tt} =$

$$\left[\left(\frac{p_{02}}{p_{01}}\right)^{\gamma/\gamma-1} - 1 \Big/ \left(\frac{T_{02}}{T_{01}} - 1\right)\right]\times 100 \quad (11)$$

Power coefficient, $\lambda = \frac{\varphi\psi}{\eta}$ (12)

SPRC $(c_p) = \frac{p_{s4}-p_{s2}}{p_{02}-p_{s2}}$ (13)

2.5 Validation of CFD Model

The simulation assumes that the flow within the diffuser path is not influenced by the relative positioning of the impeller and diffuser. The numerical model is validated against experimental data from Reddy et al. (2004) and Reddy et al., (2007). Figure 4 illustrates the relationship between the head coefficient and the normalized flow coefficient for both LSVD and VLD. As anticipated for the compressor stage, the figure shows a decrease in the head coefficient as the mass flow rate increases, a trend consistent with both experimental and numerical results.

However, the CFD simulations predict a slightly higher total head coefficient for LSVD compared to the experimental data. This discrepancy is partly due to the assumption of steady impeller-diffuser interaction in the CFD simulations, while in reality, the interaction in a centrifugal compressor stage is unsteady. This difference contributes to the higher head coefficient observed in the CFD results.

Figure 5 illustrates the relationship between the diffuser output flow angle and the normalized flow coefficient. It highlights that as the MFR increased, the exit flow angle also increased for both VLD and LSVD diffusers. In the experimental tests, flow measurements

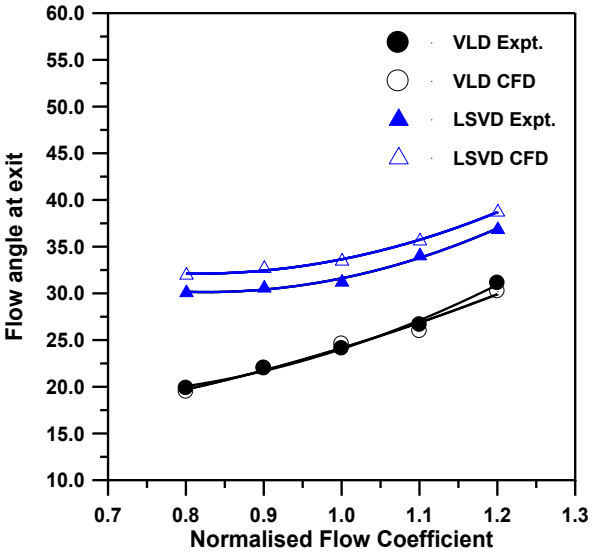

Fig. 5 Variation of diffuser exit flow angle

taken at the exits of both the impeller and diffuser showed that the flow angle could vary by 10° to 20° at a specific flow rate. This variation in flow angle was consistently observed during the experiments.

The CFD results mirrored these experimental findings, supporting the validity of the model used in the simulation. The agreement between CFD and experimental data confirms that the flow follows a logarithmic spiral path through the vaneless diffuser. This path is characteristic of how the fluid behaves within a diffuser, where the flow experiences a gradual curvature as it decelerates, which leads to changes in the flow angle.

Given the good correlation between the CFD and experimental data, the same CFD model is used for further analysis and investigation. This consistency not only validates the simulation approach but also strengthens confidence in the results for future performance predictions and diffuser design optimizations.

3. RESULTS AND DISCUSSION

Based on the numerical investigations conducted, the results are analyzed to assess the performance of the compressor stage with twisted vanes in the diffuser. Key parameters such as stage efficiency, head coefficient, power coefficient, diffuser SPR coefficient, entropy variation, and TKE variation are used to evaluate the stage performance, as detailed in the following sections. For data analysis, normalized parameters are utilized. Normalization is performed at the design point, using the data from the vaneless diffuser as a reference.

3.1 Total-to-static Stage Efficiency

Stage efficiency is employed to evaluate the performance of centrifugal compressor stages, considering the conditions at both the diffuser outlet and the impeller inlet. This approach reflects the combined performance of the impeller and diffuser. Figure 6(a) illustrates the variation in total-to-static stage efficiency for different twist angles at a fixed setup angle. Stage efficiency rose for all MFR when compared with LSVD at setting angle 16° as the twist angle increased. The decrease in secondary flows could be the cause of the efficiency gain with twist angle. The figure indicates that at 120% of the design MFR, the efficiency is lower than that of the VLD for twist angles of 5° and 7°. At the design MFR, the highest efficiency is observed across all considered twist angles. The maximum efficiency occurs for the 11° twist configuration at the design flow coefficient, which is 4.19% higher than the efficiency of the LSVD at a 16° setting angle.

When comparing LSVD NACA 0010 to setting angle 20º, all selected flow coefficients exhibit an increase in efficiency as the twist angle increases from 5º to 11º. The decrease in secondary flows could be the cause of the efficiency gain with twist angle. For 11º twist, there is a 0.81% increment at low design flow and a 4.33% increase for high design flow efficiency. The design flow point is where the maximum efficiency is seen for all twist angles taken into consideration. Efficiency increases for all selected flow coefficients at setting angle 24º when the twist angle increases from 5º to 9º in comparison to LSVD NACA 0010. However, efficiency decreases for all evaluated flow coefficients for the 11º twist, with the exception of a high flow coefficient as compared to the 9º twist. The decrease in secondary flows could be the cause of the efficiency gain with twist angle. Efficiency increases by 2.23% at high design flow and 0.68% increment is recorded for 9º twist at below design flow. The design flow point is where the maximum efficiency is seen for all twist angles. In comparison to LSVD NACA 0010, the efficiency is higher at setting angle 28º and twist angle 5º for all selected flow coefficients. However, efficiency decreases for all evaluated flow coefficients for the other twist angles, with the exception of a high flow coefficient as compared to LSVD NACA 0010. A 0.26% increment is noted for 5º twist at design flow in comparison to LSVD NACA 0010.In comparison to LSVD NACA 0010, the efficiency is higher at setting angle 32º and twist angle 5º for all selected flow coefficients. However, efficiency decreases for all investigated flow coefficients for the other twist angles. Figure 6(b) demonstrates the variation of normalized stage efficiency for different setup angles at a fixed twist. At a 5° twist angle, the stage efficiency is higher for all MFRs compared to the LSVD with the NACA 0010 airfoil at a 28° setting angle, except at the 32° setting angle. Efficiency decreases with increasing setting angle at lower flow coefficients, whereas it increases at higher flow coefficients. When compared to the LSVD at a 28° setting angle, the efficiency increases by 4.72% at 80% MFR and decreases by 10.1% at 100% MFR for a 16° setting angle.

When comparing the LSVD NACA 0010 at a 28° setting angle with a 7° twist angle, the efficiency improves for all selected flow coefficients as the setting angle increases from 16° to 24°. A similar trend is observed for a 9° twist angle, where the efficiency increases as the setting angle rises from 16° to 24° for all selected flow coefficients. However, at a 11° twist angle, the efficiency at the design flow coefficient decreases as the setting angle increases from 16° to 32°. As shown in Fig. 6(a) and (b), this trend is consistent across all twist angles. Compared

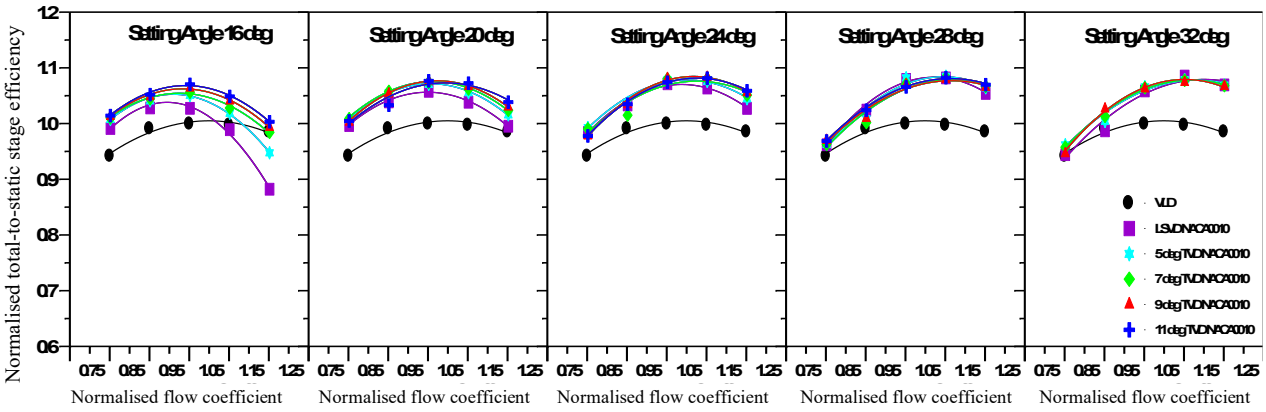

Fig. 6 (a) Variation of total-to-static stage efficiency at a given setting angle for different twist angles

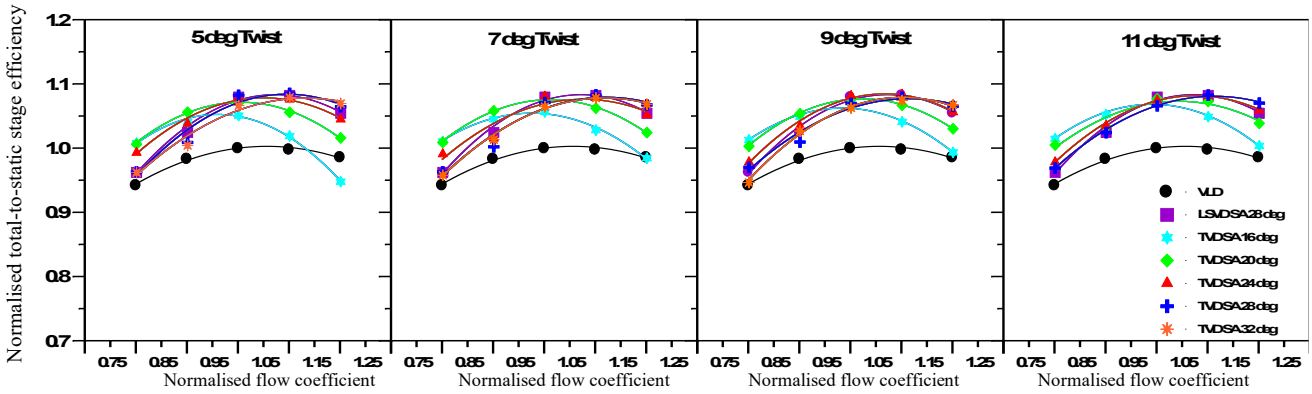

Fig. 6 (b) Variation of total-to-static stage efficiency at a given twist for different setting angles

to the LSVD, the TVD appears to offer a better surge buffer, as indicated by the steeper slopes of the curves. Therefore, twisting improves both the efficiency and the operational range of the compressor stage. The highest efficiency is reported at a 24° setting angle and a 9° twist angle.

3.2 Head Coefficient

The static head represents the increase in static pressure from the diffuser exit to the impeller inlet. Figure 7(a) and 7(b) show the variations in the normalized head coefficient with respect to the normalized flow coefficient. Figure 7(a) illustrates how the normalized static head coefficient changes with the flow coefficient for selected twist angles at a solidity of 0.81. It shows that for all low flow coefficients, the head coefficient increases at a 16° setting angle as the twist angle is increased compared to the LSVD. For high flow coefficients, the head coefficient decreases below the VLD value with a 5° twist. However, as the twist angle increases, the head rise diminishes. At an 11° twist angle, the head rise nearly matches the VLD head rise at 120% of the design MFR. The figure demonstrates that the head coefficient is improved for all TVD vane twist angles (from 5° to 11°) compared to the vaneless case for all flow coefficients studied at setting angles of 20°, 24°, and 28°. At all twist angles taken into consideration, the improvement in head coefficient is more than in the VLD example, but the increase at low flows is only slightly greater than that in the LSVD case.

The head rise improvement observed at lower flow coefficients could perhaps be attributed to decreased losses and optimal incidence caused by aligning the impeller exit flow angle with the diffuser setting angles. For all tested setting angles, the stall range with TVD vanes outperformed the vaneless case, as seen by the positive slope of the curve at low flows. This figure shows that, compared to the vaneless case, at setting angle 32º, the head coefficient has significantly improved with an increase in flow coefficient for all TVD vane twist angles from 5º to 9º. However, when compared to the LSVD at all considered twist angles, the increase in head coefficient at low MFRs is negligible. Furthermore, Fig. 7(a) shows that, unlike the vaneless diffuser, the head coefficient decreases at higher flow coefficients beyond the design threshold for the lower setting angles of 16° and 20°. In contrast, at the higher setting angles of 24°, 28°, and 32°, the head coefficient is found to be higher compared to the other settings examined at the design point. Therefore, the performance improvement observed at the higher setting angles of 24°, 28°, and 32° appears to be linked to the use of TVD. Amineni et al. (1996) demonstrated that for LSVD with constant thickness vanes and 0.7 solidity, the head drops off rapidly beyond the design point. The tip Mach number for these tests was 0.7. Even though the current CFD experiments were carried out at a Mach number of 0.35, the results indicate that using aerofoil-shaped TVD vanes can enhance the situation over a range of up to 120%.

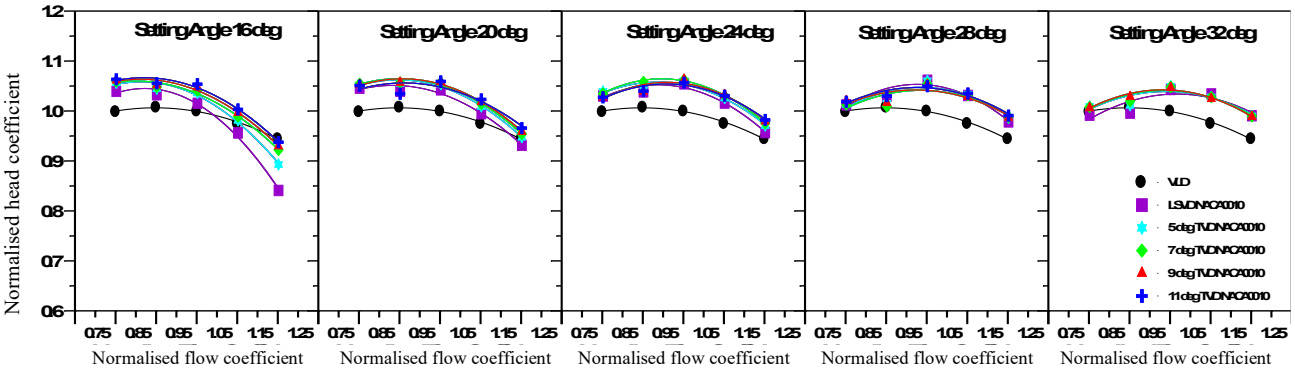

Fig. 7 (a) Variation of head coefficient at a given setting angle for different twist angles

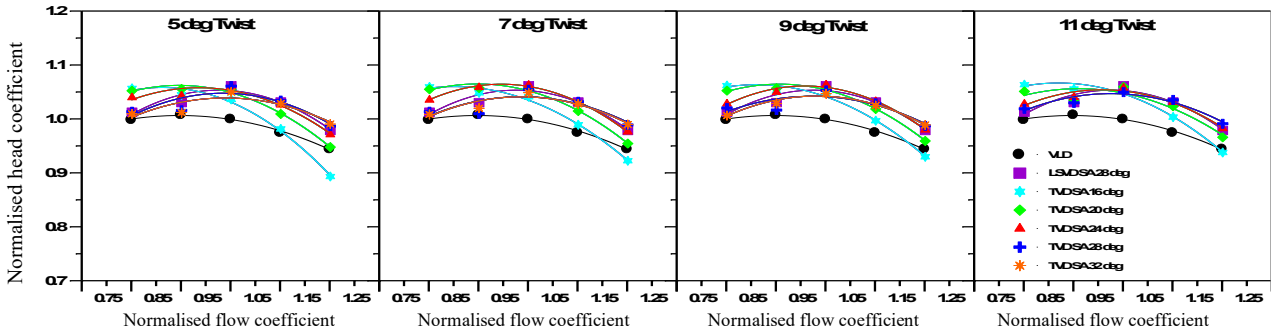

Fig. 7 (b) Variation of head coefficient at a given twist for different setting angles

Therefore, it would seem that the performance gain at high setting angles of 24 to 32 degrees with twist is mostly due to the usage of diffuser vanes with aerofoil shapes.

The normalized total head coefficient fluctuation at a given twist for various setup angles is displayed in Fig. 7(b). The figure shows that at 5º twist angle, the head coefficient across the VLD for all twist angles at lower flow rates improves noticeably as the setting angle increases. The head coefficient at 80% design flow has improved by 5.9%, 5.4%, 4.14%, 1.5%, and 1.1% with VLD for 16º, 20º, 24º, 28º, and 32º, respectively, and 4.3%, 3.9%, 2.6%, and 0.09% with LSVD NACA 0010 at setting angle 28º. In contrast, for setting angles 20º, 24º, 28º, and 32º, head coefficient improved by 0.4%, 2.8%, 4.5%, and 4.8%, respectively, with LSVD NACA 0010 at setting angle 28º. At high flow coefficient, 1.2, for setting angle 16º, head coefficient decreased below value of VLD configuration. For high flow coefficients at 24º, 28º, and 32º setting angles, the head coefficient is enhanced over LSVD NACA 0010 at 28º. The figure shows that at 7º twist angle, the head coefficient across the VLD improves significantly as the setting angle increases for all twist angles at lower MFRs. The head coefficient at 80% design flow has improved by 6.1%, 5.7%, 3.7%, 1.5%, and 1% with VLD for 16º, 20º, 24º, 28º, and 32º, respectively, and 4.6%, 4.1%, 2.2%, and 0.1% with LSVD NACA 001.

For setting angles 20º, 24º, 28º, and 32º, head coefficient improved by 1.1%, 3.4%, 4.7%, and 4.9%, respectively, with LSVD NACA 0010 at setting angle 28º, however in the case of high flow coefficient at 1.2, head coefficient decreased below the value of VLD configuration for setting angle 16º. For 24º, 28º, and 32º setting angles, the head coefficient is enhanced over LSVD NACA 0010 at 28º setting angle at high flow coefficients. When compared to the head coefficient at the 5º twist angle for the selected setting angles, the head coefficient is better at this twist angle. The figure shows that, at a twist angle of 9 degrees, the head coefficient significantly outperforms the VLD and LSVD for all twist angles at lower flow rates when the setting angle is increased. The head coefficient has improved at 80% design flow by 6.3%, 5.4%, 2.9%, 2.2%, and 0.8% with VLD for 16^0, 20º,24º, 28º, and 32º respectively, and 4.8%, 3.9%, 1.5%, and 0.7% with LSVD NACA 0010. When there is a high flow coefficient (1.2), the head coefficient at angle 16 decreases below the value of the VLD configuration; nevertheless, the head coefficient increases by 1.6%, 3.78%, 4.57%, and 4.74%, respectively, at angles 20, 24, 28, and 32.

For 24º, 28º, and 32º setting angles, the head coefficient is higher when compared to that of LSVD NACA 0010 at 28º setting angle at high flow coefficients. The figure shows that, at twist angle 11º, the head coefficient significantly improves over the VLD and LSVD for all twist angles at lower flow rates as the setting angle increases. With VLD, the head coefficient has improved by 6.5%, 5.3%, 2.9%, and 2.1% for 16^0, 20^0, 24º, 28º respectively, at 80% design flow. With LSVD NACA 0010, the improvements are 5.04%, 3.81%, 1.48%, and 0.62% for the same parameters. In the event of a high flow coefficient of 1.2, the head coefficient decreased below the VLD configuration for setting angles 16o, while head coefficients improved by 2.3%, 4%, and 4.9%, respectively, for setting angles 20^0, 24º, 28º and by 1.27% and 0.38%, respectively, for setting angles 24º and 28º,

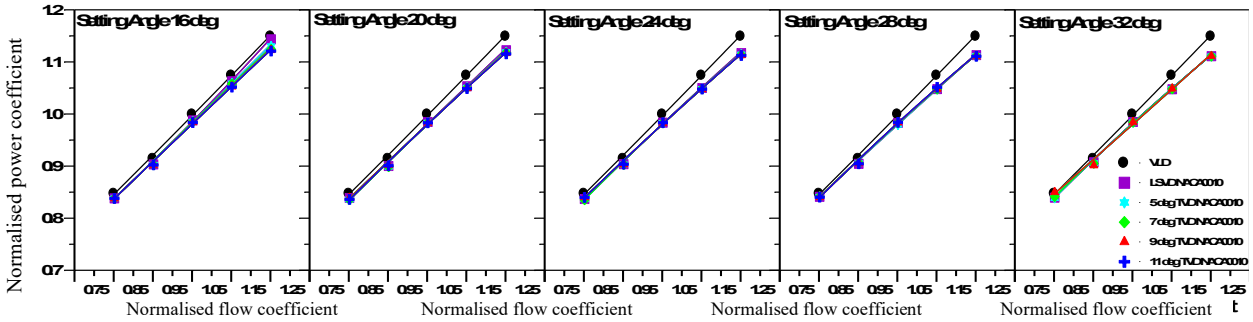

Fig. 8(a) Variation of power coefficient at a given setting angle for different twist angles

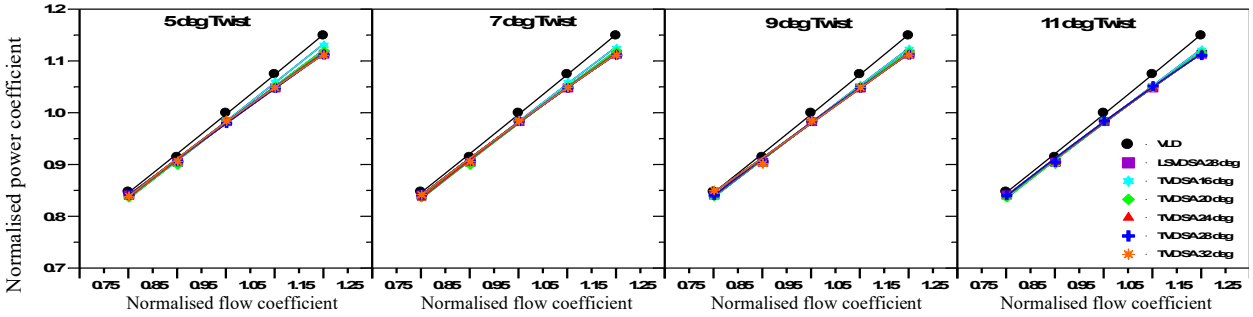

Fig. 8(b) Variation of power coefficient at a given twist for different setting angles

when compared to LSVD NACA 0010 at setting angle 28°.

3.3 Power Coefficient

Figure 8(a) presents the variation in normalized power coefficient for different twist angles at a fixed setup angle. For all low solidity diffusers, twisted vaned diffusers with various setting angles, and vaneless diffusers, the power coefficient increases consistently as the flow coefficient rises from 0.8 to 1.2 times the design flow coefficient. Throughout the study, the power coefficient variation for the VLD stage indicates higher power consumption compared to both LSVD and TVD. For a backward-curved bladed impeller, the power coefficient change follows the typical behavior associated with the limiting feature. Efficiency is inversely related to the power coefficient, while the head coefficient is proportional. When comparing the VLD, LSVD, and TVD configurations, as shown in Figs 7(a) and (b), there is a noticeable improvement in efficiency at flow coefficients above the design flow coefficient, but the head coefficient remains almost constant. Figure 8(a) shows that for both LSVD and TVD cases, the power coefficient decreases significantly as the flow coefficient increases, indicating that the increase in efficiency outweighs the impact of the head coefficient.

The normalized power coefficients for twisted vane configurations show a slight reduction of 0.31% across all flow coefficients, as depicted in the figure. The power coefficient decreases from 0.2% at 90% flow to 0.78% at 120% flow. However, at 80% flow rate, there is a small increase of 0.18% compared to the LSVD. The change in power coefficient remains minimal with twist angles ranging from 5° to 11°. Figure 8(b) illustrates the power coefficient variation at a given twist angle for different setup angles. For all diffusers, the power coefficient increases steadily as the flow coefficient rises from 0.80 to 1.20. Compared to twisted vane diffuser configurations, the LSVD has a higher power coefficient. The fluctuation in power coefficient follows the typical pattern of a backward-curved bladed impeller. Efficiency is inversely related to the power coefficient, which is directly related to the head coefficient. While efficiency significantly improves at higher flow coefficients, the head coefficient in both LSVD and TVD configurations remains nearly the same.

3.4 SPR Coefficient

The SPR coefficient (cp) represents the amount of static pressure recovered from the available dynamic head at the diffuser inlet. Figure 9(a) shows the variation of the SPR coefficient with the normalized flow coefficient at a specific setting angle for each of the configurations studied. The figure demonstrates that, when a twist is applied to all setting angles, the SPR coefficient increases significantly for low flow coefficients up to the design flow coefficient, compared to the LSVD NACA 0010. This is because lower flow angles create a larger spiral path for the fluid particles to follow, which typically leads to stalling in the vaneless diffuser passage at low flow coefficients.

For the LSVD vane configuration with a 16° setting angle, the SPR coefficient is lower than that of the vaneless diffuser case above the design flow coefficient. The reduction in SPR coefficient caused by twisting is limited to a maximum of 120% of the design MFR. As the flow exceeds the design flow, the SPR coefficient continuously decreases and shows poorer recovery compared to the vaneless diffuser case. Although the 16° setting angle demonstrates better recovery at lower flows,

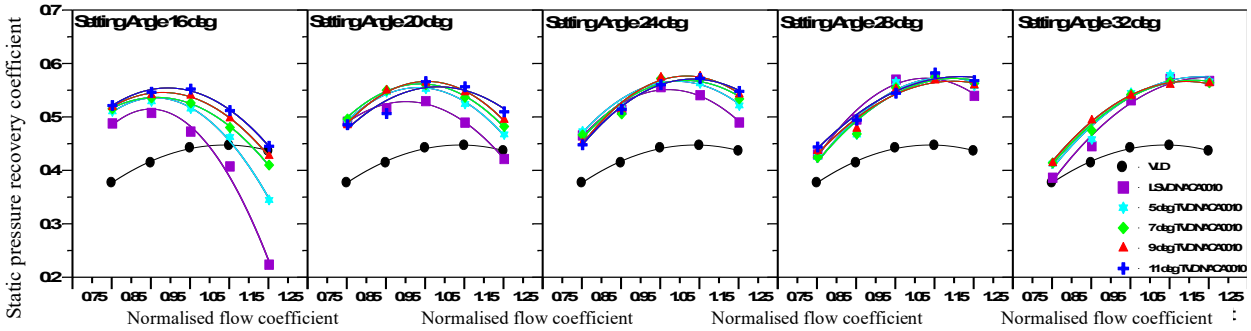

Fig. 9(a) Variation of static pressure recovery coefficient at a given setting angle for different twist angles

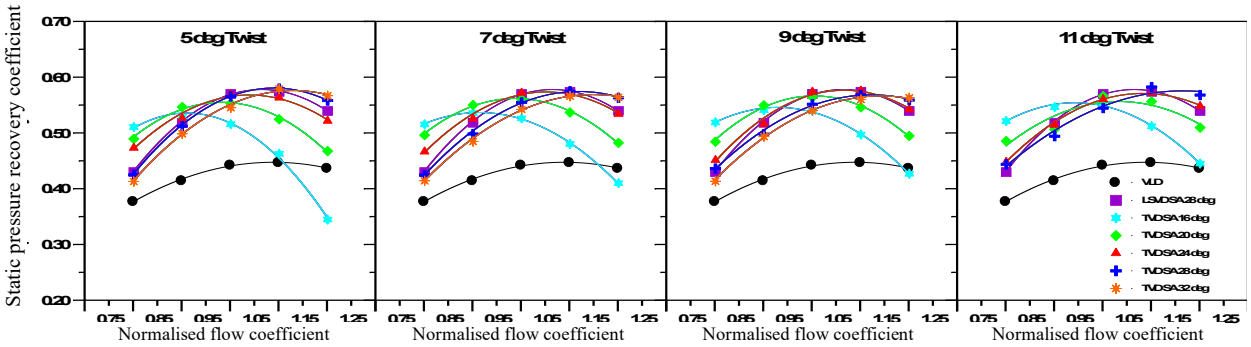

Fig. 9(b) Variation of static pressure recovery coefficient at a given twist for different setting angles

it does not appear advantageous for typical off-design operations. A similar trend is observed for the TVD with a 20° setting angle when compared to the 16° setting angle, showing comparable pressure recovery characteristics.

At a 20° setting angle, the TVD SPR coefficient is higher than that of the VLD for all the flow coefficients considered. A similar trend is observed at a 24° setting angle, where the SPR coefficient follows the same pattern as seen at 20°. The SPR coefficient increases as the twist angle is raised from 5° to 9° for all MFRs. However, at a twist angle of 11°, there is a significant decrease in the SPR coefficient at the design flow. The peak SPR is observed at the design flow for all setting angles. For a twist angle of 9°, the SPR coefficient improves consistently, ranging from 1.93% to 10.88% as the MFR increases. At the design flow, an improvement of 3.6% in the SPR coefficient is observed compared to the LSVD NACA 0010 configuration for the chosen impeller-diffuser setup. This improvement in SPR is more significant at this twist angle than at the 16° and 20° setting angles across all flow coefficients considered. Additionally, the figure indicates that the SPR improvement is more pronounced at higher flow coefficients compared to lower ones.

The pressure recovery for the TVD with 28° and 32° setting angles shows similar trends to the 24° setting angle. However, at a 28° setting angle, the TVD exhibits a lower SPR coefficient at low flow coefficients compared to high flow coefficients.

Figure 9(b) shows the variation of the SPR coefficient at a given twist for different setup angles. At a 5° twist angle, the SPR coefficient improves at higher flow coefficients as the setting angle increases. A similar trend is observed at a 7° twist angle. However, for twist angles of 9° and 11°, the SPR coefficient increases up to a setting angle of 24°, after which it starts to decrease with setting angles of 28° and 32°. When compared to the 28° setting angle across all flow rates, the TVD with a 24° setting angle and a 9° twist shows slightly better pressure recovery. Based on the current study, the TVD with a 24° setting angle and a 9° twist demonstrates superior pressure recovery compared to other configurations.

3.5 Entropy Variation

The description of Fig. 10 outlines how entropy contours are used to analyze the diffuser's exit section for different twist angles, which is crucial for understanding efficiency losses due to secondary flow generation. The figure shows entropy contours, which help visualize areas of high and low efficiency. Entropy is directly related to energy loss, so the contours highlight regions where the flow is experiencing losses. The study considers twist angles ranging from 5° to 11°, and at each twist angle, the diffuser's exit section exhibits higher entropy at the shroud compared to the hub. This suggests that secondary flows, which are typically associated with larger pressure differences or flow separations, are more pronounced near the shroud. Among the various diffuser configurations, the NACA 0010 airfoil with a 9° twist angle demonstrates the lowest maximum entropy region. This indicates that the flow through the diffuser is more efficient for this configuration, with less energy loss. Secondary flows, which can be caused by vortex formations or changes in the flow direction due to the twist, are primarily responsible for the observed efficiency losses. The NACA 0010 configuration with a 9° twist angle minimizes these secondary flows, leading to better performance in terms of entropy reduction.

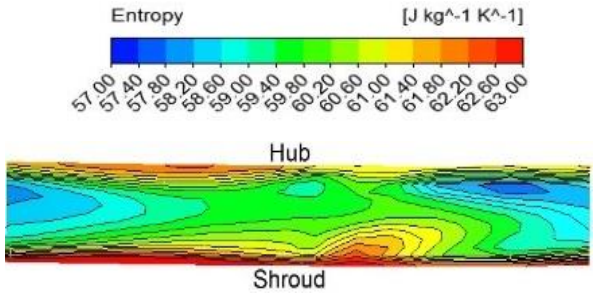

(a) Diffuser vane NACA 0010 at setting angle 24° twist

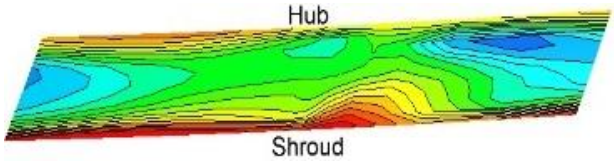

(b) Diffuser vane NACA 0010 at setting angle 24° , 5° twist

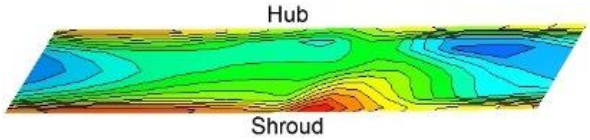

(c) Diffuser vane NACA 0010 at setting angle 24° , 7° twist

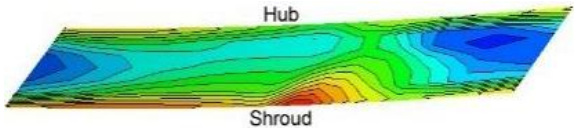

(d) Diffuser vane NACA 0010 at setting angle 24° , 9° twist

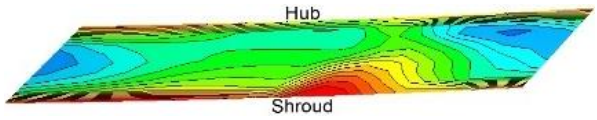

(e) Diffuser vane NACA 0010 at setting angle 24° , 11° twist

Fig. 10 Entropy contours at diffuser exit section

3.6 Turbulence Kinetic Energy (TKE) Variation

TKE serves as a crucial indicator of the turbulence intensity in the flow, influencing both heat transfer across the boundary layer and momentum exchange. Higher TKE values typically correspond to stronger turbulence, which can lead to greater instability in the flow. This instability is generally associated with less efficient flow conditions, as excessive turbulence disrupts smooth flow and can increase drag. In the analysis of the centrifugal compressor, TKE variation was studied under different flow conditions by considering contour plots (Figs 11.a to 11.c), which illustrate TKE distributions for MFRs of 80%, 100%, and 120% of the intended design MFR. These plots were examined across various twist angles ranging from 5° to 11° in 2° increments at a span of 0.5 from the hub, with the compressor setting angle fixed at 24°.

TKE increases as the flow coefficient decreases. This is attributed to the negative incidence that occurs at lower

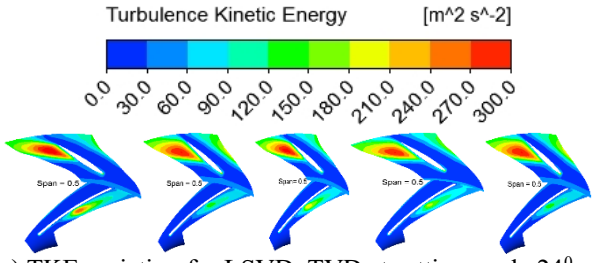

(a) TKE variation for LSVD, TVD at setting angle 24^0 and 80% of design mass flow rate

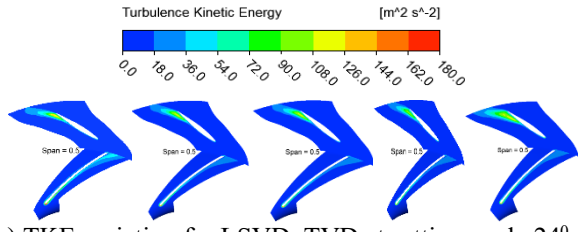

(b) TKE variation for LSVD, TVD at setting angle 24^0 and 100% of design mass flow rate

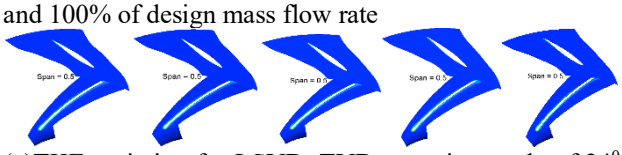

(c)TKE variation for LSVD, TVD at setting angle of 24^0 and 120%, of design mass flow rate

Fig. 11 TKE variation for LSVD, TVD

flow coefficients, which tends to generate higher levels of turbulence. In contrast, as the MFR increases, the flow stabilizes, leading to a reduction in TKE and, consequently, a more stable and efficient stage performance. Among the diffuser configurations examined, the NACA 2410 diffuser exhibited the lowest TKE across the range of MFRs studied. This suggests that the NACA 2410 diffuser configuration is particularly effective in reducing turbulence and enhancing flow stability, making it a preferred choice for maintaining high efficiency in the compressor stage.

4. CONCLUSION

Numerical simulations were conducted on a specific stage of an industrial centrifugal compressor to evaluate whether twisted vanes could improve performance compared to a low solidity vaned diffuser. The following conclusions were drawn:

1. **Improved Performance with Twisted Vanes**: The performance of the chosen compressor stage is improved by utilizing twisted diffuser vanes. The performance is significantly influenced by the twist angle. Across all flow rates analyzed, there is a consistent improvement in efficiency, head rise, and specific power ratio (SPR) with twisted vanes.
2. **Increased Range of Operation**: Twisting the diffuser blades also broadens the operational range. Compared to the low solidity vaned diffuser (LSVD), a 9° twist results in an average efficiency improvement of 1.24%. Additionally, head rise is improved by 1.52% below design flow and 2.37% above design flow. The SPR coefficient steadily

increases from 1.93% at low flow rates to 10.88% at higher flow rates, with a 3.6% improvement in SPR at design flow compared to LSVD.

3. **Minimal Impact on Power Coefficient**: The power coefficient shows a slight reduction, with an average decrease of 0.31% across all MFRs. However, entropy generation and turbulent kinetic energy (TKE) analysis highlight the superiority of the NACA 0010 configuration with a 24° setting angle and 9° twist, compared to the other configurations.
4. **Effect of Twist Angle on SPR**: For twist angles of 9° and 11°, the SPR coefficient improves up to a setting angle of 24°. However, as the setting angle increases to 28° and 32°, the SPR begins to decrease.
5. **Optimal Twist and Setting Angle**: The optimal twist angle for achieving the best performance is 9° with a setting angle of 24° for the selected impeller-diffuser configuration.

In summary, twisted diffuser vanes provide noticeable performance improvements, particularly in efficiency, head rise, and SPR, with the most favorable performance achieved at a 9° twist angle and a 24° setting angle.

ACKNOWLEDGMENTS

The authors sincerely thank the Management, Head, Mechanical Engineering Department and Principal of Vasavi College of Engineering for extending their support in carrying out this work.

FUNDING

This work received no funding

CONFLICT OF INTEREST

The authors declare that they have no conflict of interest

AUTHORS' CONTRIBUTION

Venkateswara Rao: Conceptualization, Data curation, Formal analysis, Investigation, Methodology, Resources, Software, Validation, Visualization, Writing – original draft. **Govindaraju:** Review & editing, Supervision. **Venkateswarlu:** Literature review, Formal analysis, Methodology, Resources. **Bhanu Kumari:** Literature review, Methodology, CFD simulations.

REFERENCES

Abdelwahab, A. (2005a, 6 - 9 June). *On the use of three-dimensional airfoil-shaped vaned diffusers with industrial centrifugal compressors.* 4th AIAA Theoretical Fluid Mechanics Meeting 2005, Toronto, Ontario Canada. https://doi.org/10.2514/6.2005-5196

Abdelwahab, A., & Gerber, G. (2008). A new three-dimensional aerofoil diffuser for centrifugal compressors. *Proceedings of the Institution of Mechanical Engineers, Part A: Journal of Power and Energy, 222*(8), 819-830. https://doi.org/10.1243/09576509JPE579

Abdelwahab, A., Gordon, G., & Baker, R. (2005b, August). *Leaned centrifugal compressor airfoil diffuser*. US Patent Application Disclosure 11/199254. https://patents.google.com/patent/US20070036647/ko

Abdelwahab, A., Gordon, G., & Baker, R. (2007, September). *Airfoil diffuser for centrifugal compressor.* US Patent Application Disclosure 11/903592. https://patents.google.com/patent/US20080038114A1/en

Amineni, N. K., & Engeda, A. (1997). *Pressure Recovery in low solidity vaned diffusers for centrifugal compressors.* Proceedings of the ASME 1997 International Gas Turbine and Aeroengine Congress and Exhibition. Volume 1: Aircraft Engine; Marine; Turbomachinery; Microturbines and Small Turbomachinery. Orlando, Florida, USA. https://doi.org/10.1115/97-GT-472

Amineni, N. K., Engeda, A., Hohlweg, W. C., & Direnzi, G. L. (1996). *Performance of low solidity and conventional diffuser systems for centrifugal compressors.* Proceedings of the ASME 1996 International Gas Turbine and Aeroengine Congress and Exhibition. Volume 1: Turbomachinery. Birmingham, UK. June 10–13, 1996. V001T01A052. ASME. https://doi.org/10.1115/96-GT-155

Beach, A. N., Brown, J. C., & Key, N. L. (2024). Inlet guide vane stagger effects on multistage compressor performance and stall inception. *Journal of Propulsion and Power, 40*(4), 547–554.

Engeda, A. (2001). The design and performance results of simple flat plate low solidity vaned diffusers. *Proceedings of the Institution of Mechanical Engineers, Part A: Journal of Power and Energy, 215*(1), 109-118. https://doi.org/10.1243/0957650011536471

Eynon, P. A., & Whitfield, A. (1997). The effect of low-solidity vaned diffusers on the performance of a turbocharger compressor. *Proceedings of the Institution of Mechanical Engineers, Part C: Journal of Mechanical Engineering Science, 211(5),* 325–339. https://doi.org/10.1243/0954406971522088

Hayami, H., Senoo, Y., & Utsunomiya, K. (1990). Application of a low solidity cascade diffuser to transonic centrifugal compressor. *ASME Journal of Turbomachinery, 112,* 25-29. https://doi.org/10.1115/1.2927416

Higashimori, H., Hasagawa, K., Sumida, K., & Suita, T. (2004, January). *Detailed flow study of Mach number 1.6 high transonic flow with a shock wave in a pressure ratio 11 centrifugal compressor impeller.* Turbo Expo: Power for Land, Sea, and Air (Vol.

41707, pp. 771-779). https://doi.org/10.1115/1.1791645

Issac, J. M., Sitaram, N., & Govardhan, M. (2004). Effect of diffuser vane height and position on the performance of a centrifugal compressor. *Proceedings of the Institution of Mechanical Engineers, Part A: Journal of Power and Energy, 218*(8), 647-654. https://doi.org/10.1243/0957650042584320

Larosiliere, L. M., Skoch G. J., & Prahst P. S. (1997). *Aerodynamic synthesis of a centrifugal impeller using CFD and measurements.* 33rd Joint Propulsion Conference and Exhibit AIAA–97–2878, Technical Report ARL–TR–1461. http://dx.doi.org/10.2514/6.1997-2878

Liu, S., Geng, S., Li, X., Jin, Y., & Zhang, H. (2023). Optimization design of aspect ratio and solidity of a heavy-duty gas turbine transonic compressor rotor. *Machines*, *11*(1), 82. https://doi.org/10.3390/machines11010082

Moore, J., & Moore, J. G. (1994). *Use of blade lean in turbomachinery redesign*. NASA Marshall Space Flight Center, Eleventh Workshop for Computational Fluid Dynamic Applications in Rocket Propulsion. https://ntrs.nasa.gov/api/citations/19950017205/downloads/19950017205.pdf

Osborne, C., & Sorokes, J. M. (1988). *The application of low solidity diffusers in centrifugal compressors*. Flows in Non-Rotating Turbomachinery Components, ASME FED - Vol. 69.

Reddy, S. T. C., Murty, R. G., Prasad, M. V. S. S. S. M., & Reddy, D. N. (2007). Experimental studies on the effect of impeller width on centrifugal compressor stage performance with low solidity vaned diffusers. *Proceedings of the Institution of Mechanical Engineers, Part A: Journal of Power and Energy, 221*(4), 519-533. https://doi.org/10.1243/09576509JPE373

Reddy, T. C. S., Murty, G. R., Mukkavilli, P., & Reddy, D. N. (2004). Effect of the setting angle of a low-solidity vaned diffuser on the performance of a centrifugal compressor stage. *Proceedings of the Institution of Mechanical Engineers, Part A: Journal of Power and Energy, 218*(8), 637-646. https://doi.org/10.1243/0957650042584294

Roberts, D. A., & Kacker, S. C. (2002). Numerical investigation of tandem-impeller designs for a gas turbine compressor. *Trans. ASME Journal of Turbomachinery, 124*(1), 36-44. http://dx.doi.org/10.1115/1.1413472

Senoo, Y. (1984, May). Low solidity cascade diffusers for wide flow range centrifugal blowers. *Flow in Centrifugal Compressors, VKI Lecture Series.*

Senoo, Y., Hayami, H., & Ueki, H. (1983). *Low-solidity tandem-cascade diffusers for wide-flow-range centrifugal blowers.* Proceedings of the ASME 1983 International Gas Turbine Conference and Exhibit. Volume 1: Turbomachinery. Phoenix, Arizona, USA. March 27–31, 1983. V001T01A002. ASME. https://doi.org/10.1115/83-GT-3

Venkateswara Rao, P., & Ramana Murty, G. V. (2013a December 12-14,). *Effect of twist in a diffuser vane on the performance of a centrifugal compressor stage.* Proceedings of the Fortieth National Conference on Fluid Mechanics and Fluid Power. NIT Hamirpur, Himachal Pradesh, India. pp.1376-1385. ISBN: 978-93-82880-90-5

Venkateswara Rao, P., Ramana Murty, G. V., & Venkata Rao, G. (2013b, November 7-8). *Performance analysis of a centrifugal compressor stage with constant thickness twisted vane diffuser*. Proceedings of the 4th National Conference on Advances in Mechanical Engineering (AIM 2013), Vasavi College of Engineering, Hyderabad, AP., 2013. pp.237-244. ISBN: 978-93-82570-16-5

Venkateswara Rao, P., Ramana Murty, G.V., & Venkata Rao, G. (2014a). Numerical studies of twisted vaned diffuser on the performance of a centrifugal compressor stage. *Universal journal of Mechanical Engineering, 2*, 163-168. https://doi.org/10.13189/ujme.2014.020503

Venkateswara Rao, P., Ramana Murty, G.V., & Venkata Rao, G. (2014b, June 16–20). *Performance comparison of twisted low solidity vaned diffusers with different shapes.* Proceedings of ASME Turbo Expo 2014: Turbine Technical Conference and Exposition, GT2014, Düsseldorf, Germany. https://doi.org/10.1115/GT2014-26833

Wu, Y., Li, Q., Yuan, H., Li, Z., Zhou, S., Han, G., & Lu, X. (2024). Performance improvement of a high loading centrifugal compressor with vaned diffuser by hub contour optimization. *Aerospace*, *11*(4), 246. https://doi.org/10.3390/aerospace11040246

Yang, X. X., & Liu, Y. (2023). A Novel Vane-twisted conformal diffuser for compact centrifugal compressors. *Journal of Applied Fluid Mechanics*, *16*(9), 1839-1852. https://doi.org/10.47176/jafm.16.09.1808

Zangeneh, M. (1991). A Compressible 3D Design method for radial and mixed flow turbomachinery blades. *International Journal for Numerical Methods in Fluids, 13(5),* 599-624. https://doi.org/10.1002/fld.1650130505

Zangeneh, M. (1998). *On 3D inverse design of centrifugal compressor impellers with splitter blades.* 43rd ASME International Gas Turbine and Aero-engine Congress and Exposition, Stockholm, Sweden, ASME paper 98-GT-507. https://doi.org/10.1115/98-GT-507